3D MHD Turbulence with a Mean Magnetic Field*

S. Oughton[1], W. H. Matthaeus[2], and E. R. Priest[1]

[1]*Department of Mathematical and Computational Sciences, The University, St Andrews, KY16 9SS, Scotland*

[2]*Bartol Research Institute, Sharp Lab, University of Delaware, Newark, DE 19716, USA*

Abstract

Building on results from two-dimensional magnetohydrodynamic (MHD) turbulence, the development of anisotropic states from initially isotropic ones is investigated numerically for fully three-dimensional incompressible MHD turbulence. It is found that when an external dc magnetic field ($\mathbf{B}_0$) is imposed on viscous and resistive MHD systems, excitations are preferentially transferred to modes with wavevectors perpendicular to $\mathbf{B}_0$. The anisotropy increases with increasing mechanical and magnetic Reynolds numbers, increasing wavenumber, and also increasing $\mathbf{B}_0$. However, for $B_0 \gtrsim 3$ the anisotropy appears to saturate. The tendency of $\mathbf{B}_0$ to inhibit development of turbulence is also examined.

1 Introduction

Previous studies of incompressible 2D MHD turbulence with an externally imposed dc magnetic field ($\mathbf{B}_0$) showed that initially isotropic turbulent states evolve into anisotropic ones in a few large-scale eddy-turnover times (Shebalin et al., 1983, hereafter SMM). Excitations were preferentially transferred to the modes with wavevectors ($\mathbf{k}$) perpendicular to $\mathbf{B}_0$, relative to the parallel modes. Since many geo- and astrophysical plasmas may be fruitfully treated as MHD fluids containing a large-scale magnetic field which varies 'slowly' on length and time scales of dynamical importance, it is of interest to consider approximations to such systems. Here we report on an extension of SMMs 2D results to three dimensions.

Specifically, we performed numerical simulations of the fully 3D incompressible MHD equations with turbulent initial conditions. For a given initial condition several runs were performed, each with a different value of B_0. We take $\mathbf{B}_0 = B_0\,\hat{\mathbf{z}}$ where B_0 is a uniform constant. The code is based on a dealiased spectral Galerkin algorithm (Orszag & Patterson, 1972; Canuto et al., 1988). In x-space the computational domain is a periodic cube of side 2π so that the wavevectors have integer components. The equations solved are (where the variables have their usual meanings):

$$\frac{\partial \mathbf{v}}{\partial t} + \mathbf{v}\cdot\nabla\mathbf{v} = -\nabla p^* + \mathbf{b}\cdot\nabla\mathbf{b} + \mathbf{B}_0\cdot\nabla\mathbf{b} + \nu\nabla^2\mathbf{v}, \tag{1}$$

$$\frac{\partial \mathbf{b}}{\partial t} + \mathbf{v}\cdot\nabla\mathbf{b} = \mathbf{b}\cdot\nabla\mathbf{v} + \mathbf{B}_0\cdot\nabla\mathbf{v} + \eta\nabla^2\mathbf{b}, \tag{2}$$

$$\nabla\cdot\mathbf{v} = 0, \qquad \nabla\cdot\mathbf{b} = 0, \tag{3}$$

Note that $\langle\mathbf{v}\rangle = \langle\mathbf{b}\rangle = 0$, where the angle brackets indicate spatial averaging. The electric current density is $\mathbf{j} = \nabla\times\mathbf{b}$, the fluid vorticity $\boldsymbol{\omega} = \nabla\times\mathbf{v}$, and of course the magnetic vector potential is related to the field by $\mathbf{b} = \nabla\times\mathbf{a}$. The kinetic and magnetic energies per unit mass are $E^v = \langle\mathbf{v}^2/2\rangle$, and $E^b = \langle\mathbf{b}^2/2\rangle$, and the three rugged invariants of ideal 3D MHD—namely, total energy, cross helicity, and magnetic helicity—are defined as $E = E^v + E^b$, $H_c = \langle\mathbf{v}\cdot\mathbf{b}\rangle/2$, and $H_m = \langle\mathbf{a}\cdot\mathbf{b}\rangle/2$, respectively (e.g., Zhou & Matthaeus, 1990). Both the bulk values of E, E^v, etc, and also their spectra $E(k)$, etc will be used. The spatial and (discrete) Fourier representations of the velocity field are related by $\mathbf{v}(\mathbf{x},t) = \sum_{\mathbf{k}}\mathbf{v}(\mathbf{k},t)\,e^{i\mathbf{k}\cdot\mathbf{x}}$, where $\mathbf{k}$ is the wavevector conjugate to $\mathbf{x}$ and having magnitude $k = |\mathbf{k}|$. Analogous expansions hold for the other fields.

*In *Current Topics in Astrophysical and Fusion Plasma Research*, Proceedings of the International Workshop on Plasma Physics, 28 Feb–5 Mar, 1994, Pichl/Schladming, Austria. M.F. Heyn, W. Kernbichler, and H.K. Biernat (eds). ISBN 3-7041-0218-0. dbv-Verlag Graz.

Initial conditions for all runs were such that $H_m \approx 0$, $E = 1$, and the Alfvén ratio, $r_A(k) = E^v(k)/E^b(k)$, was unity for each excited mode. Each run had a resolution of 64^3, and $\nu = \eta = \frac{1}{200}$. Five values of B_0 were used: 0, 0.1, 1, 3, and 8. In the following section we report on some results from the simulations and then close with a short discussion and summary. A more complete discussion of these results is to be found in Oughton et al. (1994).

2 Results

In this section we first present some results regarding bulk parameters of the flows and then turn to anisotropy diagnostics. Most of the features and trends pointed out in this section were also seen in SMMs 2D study. Time histories of the globals show qualitatively similar behaviour across runs; however, at least three trends are evident (Figure 1). First, the energy plots show that increasing B_0 tends to make E^v and E^b more nearly equal; i.e., it better enforces $r_A = 1$, *à la* the Alfvén effect (Kraichnan, 1965; Pouquet et al., 1976). Second, the maxima in the enstrophy, $\Omega = \langle\, \boldsymbol{\omega}^2 \,\rangle/2$, and the mean square current density, $J = \langle\, \mathbf{j}^2 \,\rangle/2$, decrease as B_0 increases, suggesting that B_0 acts to suppress or inhibit the turbulence (see next section). Note that Ω and J are plotted using the same vertical scaling to better emphasize their differences when $B_0 = 0$ and 1, and their similarities when $B_0 = 3$. The third trend is that the time histories display more structure (or 'fast' fluctuations) as B_0 is increased, this being particularly noticable for $\langle a^2 \rangle/2$ which is the lowest k-moment sum shown. This suggests that there may be an increased wavelike/oscillatory contribution in such quantities.

To quantify the degree of anisotropy associated with a flow, we introduce the generalized Shebalin (SMM) angles, θ_Q, defined by

$$\tan^2 \theta_Q \;=\; \frac{\Sigma\, k_\perp^2 |\mathbf{Q}(\mathbf{k},t)|^2}{\Sigma\, k_z^2 |\mathbf{Q}(\mathbf{k},t)|^2}, \tag{4}$$

where $k_\perp^2 = k_x^2 + k_y^2$, $\mathbf{Q}$ is any one of the vector fields $\boldsymbol{\psi}$, $\mathbf{v}$, $\boldsymbol{\omega}$, $\mathbf{a}$, $\mathbf{b}$, $\mathbf{j}$, and the summations extend over all values of $\mathbf{k}$. Physically, $\tan^2 \theta_Q$ is interpretable as the ratio of a weighted mean-square perpendicular wavenumber to its parallel counterpart, the weighting factor being the 'energy' spectrum for $\mathbf{Q}$. Thus, an isotropic spectrum corresponds to $\theta_Q = \tan^{-1}\sqrt{2} \simeq 54.74^\circ$, while a spectrum having all its energy in modes perpendicular to $\mathbf{B}_0$ has $\theta_Q = 90^\circ$. As a shorthand we will speak of Q increasing or decreasing, where we define the orderings as $\psi < v < \omega$ and $a < b < j$.

Figure 2 shows plots of $\theta_Q(t)$ for each field, each curve corresponding to a different value of B_0. Fluctuations in the angles are evident, but their initial behaviour when $B_0 \gtrsim 1/2$ is characterised by a more or less steady increase with time. At later times, and when $B_0 \gtrsim 1$, most of the angles attain approximately constant values, but note that the time taken to reach the plateaus appears to depend on both Q and B_0. It is also evident that the degree of anisotropy increases with B_0, at least for $B_0 \lesssim 3$. Further increases in B_0 result in essentially the same anisotropy levels. A minimum value of B_0 below which the anisotropy does not develop is also suggested by Figure 2.

Consider the runs individually for the moment. Note the usual ordering of the angles when $B_0 \gtrsim 1/2$; namely $\theta_\psi < \theta_v < \theta_\omega$ and $\theta_a < \theta_b < \theta_j$, as also noted by SMM. They attributed the trend to increased anisotropy at higher wavenumbers. The idea is that since $\mathbf{v}$ has a stronger dependence on the small-scales than $\boldsymbol{\psi}$, and $\boldsymbol{\omega}$ a still stronger dependence, larger anisotropies for higher wave-numbers will tend to give the observed orderings. Stated briefly, *anisotropy increases as Q does* (for a given B_0).

The stronger dependence on small-scale structure for θ_ω and θ_j may also explain why (for large B_0) these angles reach their plateau levels faster than the lower Q ones, despite having to achieve larger values: higher k-modes have shorter characteristic times and can thus achieve 'equilibrium' values faster than lower ones. For the $B_0 = 3$ and 8 runs, the v-b and ω-j angles level out at $t \approx 4$, whereas the ψ-a angles have apparently not done so by $t = 8$. Furthermore, comparing only the rapid rise portions of the curves, the ω-j angles reach 70° in half the time it takes for the v-b angles to do so.

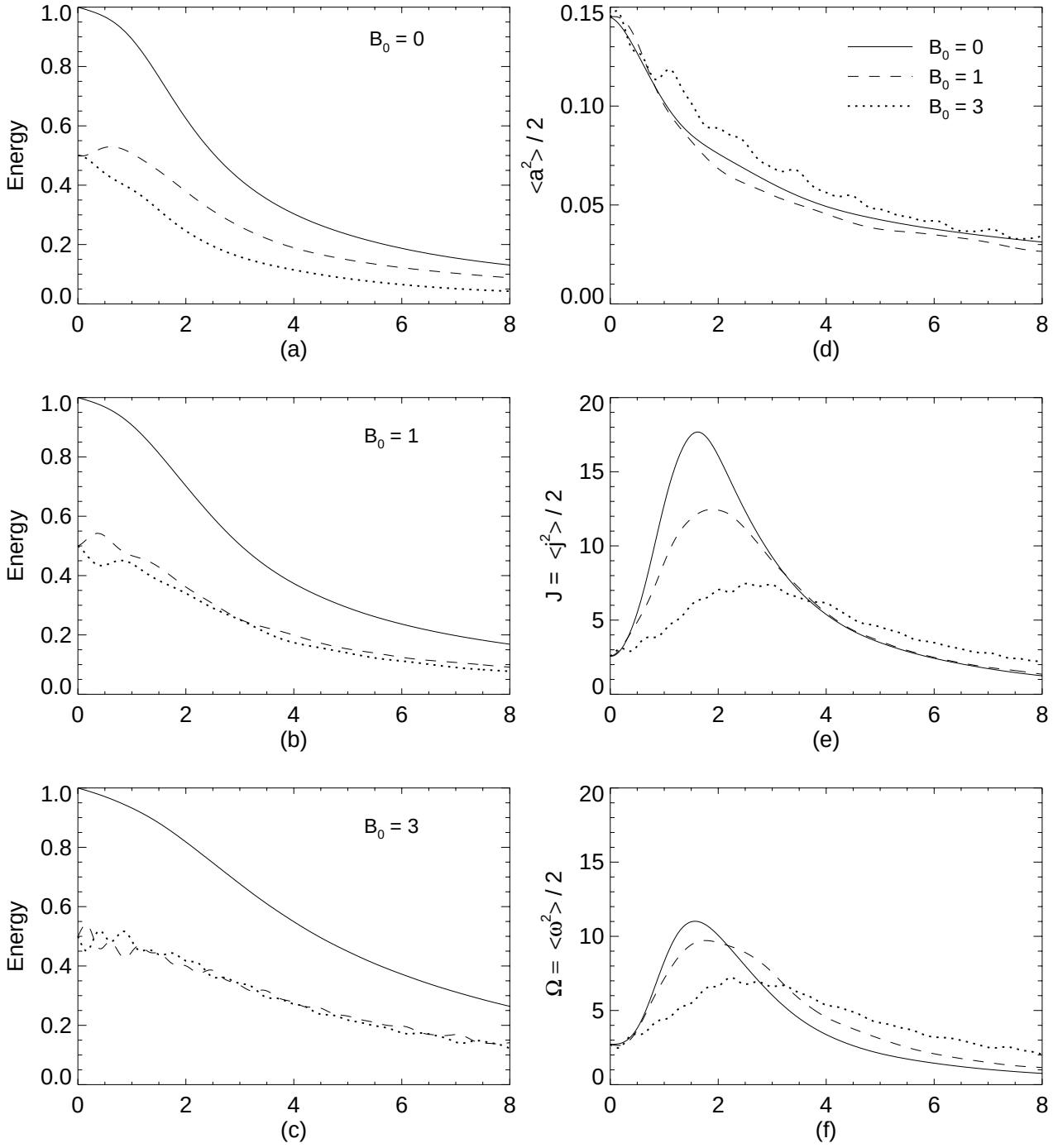

Figure 1: Time histories of some bulk quantities for the $B_0 = 0, 1$, and 3 runs ($\nu = \eta = 1/200$): (a)–(c) energies for each run, (d) mean square vector potential, (e) mean square current density, (f) enstrophy. The horizontal coordinate is time.

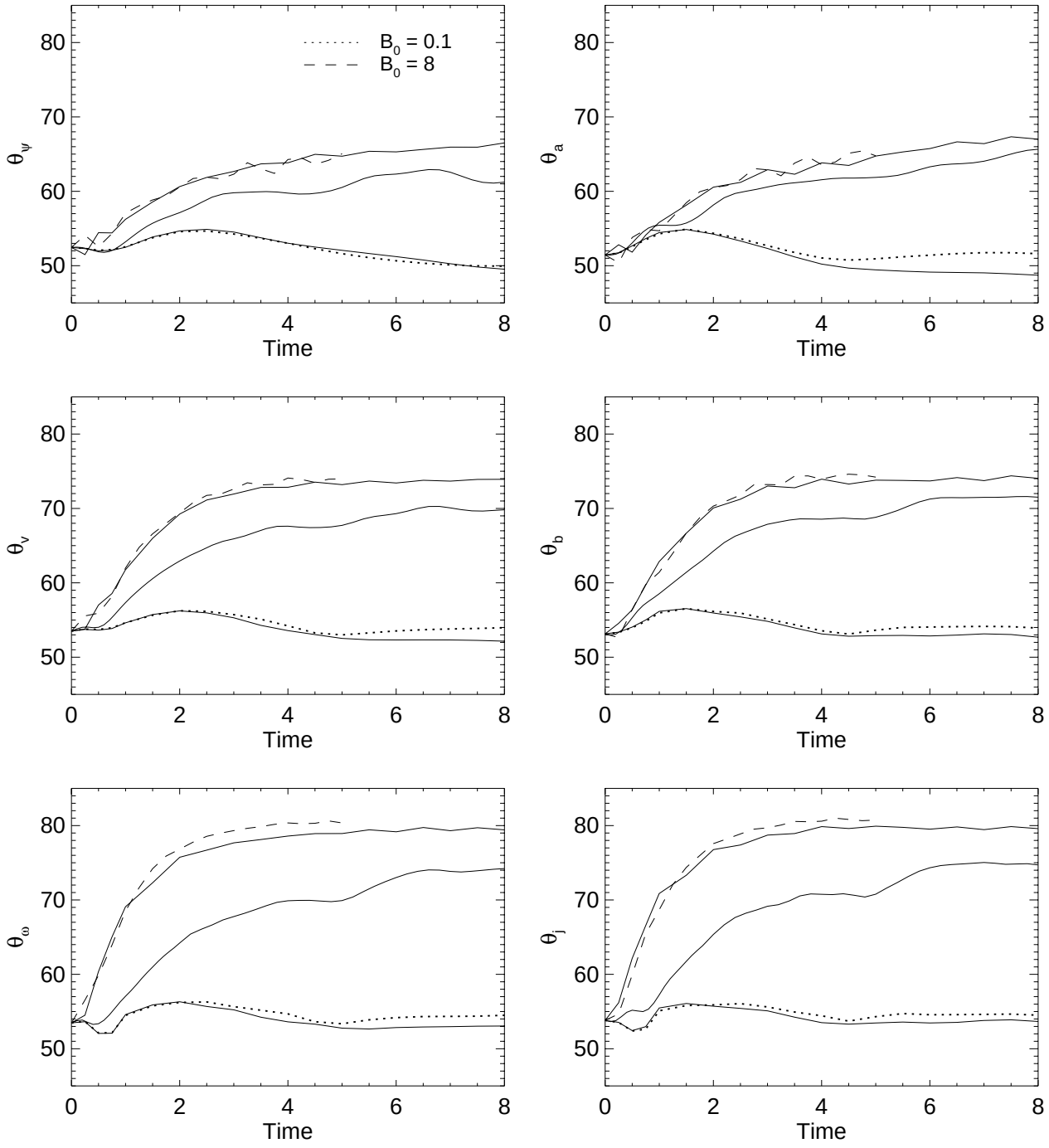

Figure 2: Generalized Shebalin angles as a function of time and B_0. Each curve corresponds to a distinct value of B_0. In general stronger anisotropies correspond to larger B_0; however, where ambiguity is possible (i.e., $B_0 = 0, 0.1$ and $B_0 = 3, 8$) unique linestyles are used as shown in the legend. Angles are in degrees.

However, we cannot be certain that such behaviour will also occur at much higher (i.e., more realistic) Reynolds numbers.

Other runs not discussed here (see Oughton et al., 1994) suggest that the anisotropies also increase with increasing Reynolds numbers. Note, however, that the anisotropies are not sustained if $\nu = \eta = 0$. Dissipation is crucial to the nonlinear process which causes the anisotropies (SMM). Finally, plots (not shown) of angles reflecting anisotropies in the the x–y plane suggest that, on average, there are none. This is in accord with the equations of motion which do not indicate any symmetry breaking in this plane.

3 Summary and Discussion

We have found that a dc magnetic field ($\mathbf{B}_0$) imposed on 3D MHD turbulent flows induces enhanced transfer of excitations to perpendicular modes, relative to parallel ones. This anisotropy, as measured by ratios of correlation lengths, tends to increase with

(i) B_0 (saturation occurring for a value $\gtrsim 3$),
(ii) wavenumber (power of k in Q),
(iii) Reynolds numbers, and
(iv) time (with a saturation depending on Q and the Reynolds numbers).

This behaviour is in almost complete qualitative agreement with the 2D results of SMM. The slight discrepancy concerns the value of B_0 at which anisotropy saturation occurs. While this 'critical' value is not determined precisely in either investigation, the 3D value is almost certainly greater than the 2D one. Given that there is an additional perpendicular degree of freedom in the 3D geometry, this seems quite reasonable.

SMM gave a physically appealing explanation for the development of the anisotropy based on a weak turbulence analysis of the dynamical equations (i.e., they computed the first order nonlinear corrections to the solutions of the linearized equations). Briefly, they showed that two excited Fourier modes ($\mathbf{k}_1$ & $\mathbf{k}_2$) will resonate effectively with a third, initially unexcited mode, only if the excited modes are oppositely propagating and satisfy certain matching conditions. The matching conditions require that either $\mathbf{k}_1$ or $\mathbf{k}_2$ is completely perpendicular to $\mathbf{B}_0$. It follows that the wavevector for the newly excited mode can have an increased perpendicular component (relative to $\mathbf{k}_1$ and $\mathbf{k}_2$), but not an increased parallel component. Hence such excitations may readily transfer energy perpendicular to $\mathbf{B}_0$ in k-space, but not parallel to it. The argument readily generalises to the 3D case.

The reasons for the anisotropy saturations with B_0 and time are unclear to us. The latter may be a consequence of the low Reynolds numbers used here. For example, if the flows were fully turbulent for say 20 characteristic times instead of ≈ 3, saturation with time might occur at both a later time and a higher level. In other words, the lack of sustained turbulence in the flows may be prematurely curtailing the degree of anisotropy which develops. The saturation with B_0 is perhaps more fundamental, and may be related to the relatively decreased strength of the nonlinear couplings at high B_0. Note that the weak turbulence explanation for the anisotropy does not depend on the strength of B_0 (provided it is strong enough to validate the approximation in the first place).

Obviously the factors considered above are not the only ones which can influence development of anisotropy. Space does not permit decent discussion regarding other factors (e.g., Alfvén ratio, various helicities), but in general non-zero values of quantities which reduce the strength of the nonlinear couplings (e.g., cross and kinetic helicity) can be expected to also reduce the level of anisotropy relative to the baseline flows of the kind discussed here (Oughton et al., 1994).

The applied B_0 also affects the level of turbulence in the flows, by reducing the relative strength of the nonlinear couplings. The maxima of the enstrophy, Ω, and the mean square current density, J, decrease essentially monotonically as B_0 increases (*cf.* Figure 1). Since growth of Ω and J is an indicator of the degree of turbulence developed in the flow, the decreasing maxima suggest that a

dc magnetic field suppresses turbulence ever more strongly as its strength increases. In fact, naive examination of the equations of motion indicates that when B_0 is large the linear terms dominate the nonlinear ones, leading to the well known result that $\mathbf{v}$ and $\mathbf{b}$ obey wave equations. However, this is not the whole story since the approximation fails to correctly account for the different perpendicular and parallel correlation lengths induced by B_0.

Frisch *et al.* noted that a sufficiently strong $\mathbf{B}_0$ leads to suppressed development of small-scale structures in that direction. They conjectured that this was a consequence of the lack of X-type neutral points in such flows, such sites being associated with intense generation of small-scale structures (e.g., $\boldsymbol{\omega}$ and $\mathbf{j}$). Whatever the reason, it does not follow that complete suppression of the turbulence ensues for large enough $\mathbf{B}_0$. By analogy with neutral fluid flows, where strong rotation can induce two-dimensionality of the flow (with respect to the rotation axis), it is physically plausible that an applied $\mathbf{B}_0$ might do likewise for magnetofluids (e.g., Cowling, 1958). In other words, the initially 3D MHD turbulence could be reduced to largely decoupled planes of 2D MHD turbulence, oriented perpendicular to $\mathbf{B}_0$. Our results are consistent with such behaviour (e.g., isotropy in the $\perp$ plane, parallel correlation lengths $\gg$ than $\perp$ ones). We should also note that recent work on nearly incompressible MHD (Zank & Matthaeus, 1992a,b, 1993) shows that in the limit of strong $\mathbf{B}_0$, the compressible 3D MHD equations reduce to incompressible 2D equations similar to those just discussed. Thus, (a) physically based arguments, (b) mathematical theorems and results, and (c) numerical simulations all indicate or suggest the same behaviour. Just how important $\mathbf{B}_0$'s suppression of turbulence is in high Reynolds number flows (forced and unforced) remains to be determined.

Acknowledgments

Troy Stribling wrote the initial version of the code in collaboration with WHM. This work was supported by the UK SERC, and the SPTP at Bartol. Computations were performed using the Cray Y/MP at the San Diego Supercomputing Centre, and workstations at St Andrews and Bartol.

References

[1] C. Canuto, M. Y. Hussaini, A. Quarteroni, and T. A. Zang. *Spectral Methods in Fluid Mechanics.* Springer Series in Computational Physics. Springer-Verlag, 1988.

[2] T. G. Cowling. *Magnetohydrodynamics.* Interscience, 1957.

[3] U. Frisch, A. Pouquet, P.-L. Sulem, and M. Meneguzzi. The dynamics of two-dimensional ideal mhd. *J. de Mécanique Théorique et Appliquée*, **216**:191, 1983.

[4] R. H. Kraichnan. Inertial-range spectrum of hydromagnetic turbulence. *Phys. Fluids*, **8**:1385, 1965.

[5] S. A. Orszag and G. S. Patterson. Numerical simulation of three dimensional homogeneous isotropic turbulence. *Phys. Rev. Lett.*, **28**:76, 1972.

[6] S. Oughton, E. R. Priest, and W. H. Matthaeus. The influence of a mean magnetic field on three-dimensional mhd turbulence. *J. Fluid Mech.*, submitted, 1994.

[7] A. Pouquet, U. Frisch, and J. Léorat. Strong mhd helical turbulence and the nonlinear dynamo effect. *J. Fluid Mech.*, **77**:321, 1976.

[8] J. V. Shebalin, W. H. Matthaeus, and D. Montgomery. Anisotropy in mhd turbulence due to a mean magnetic field. *J. Plasma Phys.*, **29**:525, 1983.

[9] G. P. Zank and W. H. Matthaeus. The equations of reduced magnetohydrodynamics. *J. Plasma Phys.*, **48**:85, 1992a.

[10] G. P. Zank and W. H. Matthaeus. Waves and turbulence in the solar wind. *J. Geophys. Res.*, **97**:17189, 1992b.

[11] G. P. Zank and W. H. Matthaeus. Nearly incompressible fluids II: Magnetohydrodynamics, turbulence, and waves. *Phys. Fluids A*, **5**:257, 1993.

[12] Y. Zhou and W. H. Matthaeus. Transport and turbulence modeling of solar wind fluctuations. *J. Geophys. Res.*, **95**:10291, 1990.